Development and Evaluation of Dependency of Flow Rate on Differential Pressure Evaluation Device

Akira Iizuka[1, a], Ronald M Galindo[2, b], Edwin Carcasona[3, c], Kenji Amagai[1, d], Akihiro Takita[1, e], Yusaku Fujii[1, f *]

[1]Gunma University Faculty of Science and Engineering 1-5-1 Tenjincho, Kiryu City, Gunma Prefecture 376-8515, Japan

[2]Faculty of Engineering, Cebu Technological University, Cebu, Philippines

[3]Faculty of Engineering, University of San Carlos, Cebu, Philippines

* Corresponding author

[a]<t231b602@gunma-u.ac.jp>, [b]<ronald.galindo@ctu.edu.ph>, [c]<edcarc123055@yahoo.com>, [e]<amagai@gunma-u.ac.jp> [e]<takita@gunma-u.ac.jp>, [f]<fujii@gunma-u.ac.jp>

Keywords: Leakage evaluation, Flow evaluation, Permeation flow rate

Abstract. The authors have developed a device for evaluating the "differential pressure dependence of the flow rate through a nonwoven fabric filter" called the "The Permeation Evaluator". "The Permeation Evaluator" consists of a pressure buffer set at a negative pressure by an exhaust fan, a fixture for attaching a filter to be measured, a differential pressure sensor, and a Flow-meter. "The Permeation Evaluator" can measure the relationship between the transmission flow rate and differential pressure of filters used in face masks and other products. The leakage flow rate of the device was measured at a differential pressure of 0 [Pa] ~ 500 [Pa], and the leakage flow rate was expressed by the estimation equation $\boldsymbol{Q} = 0.00033\,\boldsymbol{\Delta P}$ with a standard uncertainty of 0.20. This value indicates the degree of leakage flow of the device. "The Breathing air simulator" consisting of a manually operated piston-cylinder mechanism (capacity : 1.75 [L]) and a Flow-meter was developed as an option to provide a disturbance flow rate to the "The Permeation Evaluator". "The Breathing air simulator" was connected to the "The Permeation Evaluator" and a disturbance flow rate was applied to the pressure buffer while changing the speed at which the piston was moved, and the degree of agreement between the applied disturbance flow rate $\boldsymbol{Q_2}$ and the exhaust flow rate $\boldsymbol{Q_1}$ from the pressure buffer was measured. The RMS value of $[\boldsymbol{Q_1} - \boldsymbol{Q_2}]/\boldsymbol{Q_1}$ was obtained. The results were as follows. When the piston was moved at high speed (1±0.1 [s]), the values were 21 [%] in the Exhaust section and 24 [%] in the Intake section. When the piston was moved at middle speed (2±0.1 [s]), the values were 16 [%] in the Exhaust section and 13 [%] in the Intake section. When the piston was moved at low speed (3±0.1 [s]), the values were 11 [%] in the Exhaust section and 9.2 [%] in the Intake section. These values indicate the reliability of the flow measurement. The analysis was performed in the range of $|\boldsymbol{Q_1}| > 10$ [L/min] in the Exhaust and Intake operation sections.

1. Introduction

COVID-19, which has ravaged the world for more than three years, seems to be coming under control. However, the possibility of a pandemic caused by a new COVID-19 mutant or a new airborne virus has not disappeared, and uncertainty is expected to continue. [1] As in the case of COVID-19, the first key item in the event of a new pandemic would be masks, such as non-woven masks and medical face masks. These masks use non-woven filters. [2] Non-woven filters are also used in medical Powered Air-Purifying Respirator (PAPR) as air purification devices. [3]

The author's research group is developing a free-air mask as a PAPR suitable for use by the general public as an alternative to viral lockdown. Non-woven filters are also used in the Intake unit [4] and Exhaust unit [5] of the "Distancing-Free Mask". [6-9]

The authors are developing a high-performance, low-cost PAPR "Distancing-Free Mask" as an alternative to lockdown. "The Permeation Evaluator" was developed for basic performance tests of a Distancing-Free Mask. "The Permeation Evaluator" is capable of accurately measuring the flow differential pressure dependence of the air supply and exhaust units of a Distancing-Free Mask.[10] Furthermore, the operation of the "Distancing-Free Mask" can be simulated by simulating the inside of the hood of the "Distancing-Free Mask" by the pressure buffer section and by attaching an air supply unit and an exhaust unit to the pressure buffer section. Furthermore, by connecting a "The Breathing air simulator" the supply and exhaust conditions of the "Distancing-Free Mask" can be simulated under the condition that the respiratory flow is given.

There are commonly available devices that can measure the "Air flow resistance" of non-woven filters.[11]

"The Permeation Evaluator" and "The Breathing air simulator" were developed for component evaluation and control algorithm development suitable for free-air mask development. No other device can measure the performance of the air supply and exhaust units of a free-air mask like "The Permeation Evaluator". In particular, no other device can simulate the operation of a free-standing mask with added breathing airflow using "The Breathing air simulator".

In this study, we developed a "The Permeation Evaluator" and a "The Breathing air simulator" connected to the device, and evaluated their performance. "The Permeation Evaluator" is a device for measuring the relationship between the transmission flow rate (Air leaking through gaps in equipment) and differential pressure of filters, such as non-woven filters used in general-use facemasks and medical-use facemasks, and commercially available unprocessed non-woven filters. "The Breathing air simulator" is a device that is connected to the "The Permeation Evaluator" to supply and exhaust air to the "The Permeation Evaluator".

The differential pressure dependence of the leakage flow rate of "The Permeation Evaluator" was evaluated when the air inlet of the device was blocked as an evaluation index of "The Permeation Evaluator". From the measurement results, we attempted to develop an estimation equation. Furthermore, "The Breathing air simulator" was connected to the "The Permeation Evaluator" and a disturbance flow (Air added from "The Breathing air simulator" to "The Permeation Evaluator") rate was applied to the pressure buffer while changing the speed at which the piston was moved, and the degree of agreement between the given disturbance flow rate $\boldsymbol{Q_2}$ and the exhaust flow rate $\boldsymbol{Q_1}$ from the pressure buffer was measured.

2. Development of "The Permeation Evaluator"

Figure 1 shows a photograph and schematic diagram of "The Permeation Evaluator". "The Permeation Evaluator" places the object to be measured (non-woven filter) between the plates (two aluminum plates with φ80 [mm] holes) and activates the exhaust fan (Model: San Ace B97 model 9BMB12P2K01, manufacture: Sanyo Electric) at the top of the device. The air that has permeated through the object to be measured (non-woven fabric filter) enters the pressure buffer, passes through Flow-meter 1, and is discharged from the exhaust fan. The device is equipped with a Flow-meter 1 (Model: SFM3000-200-C, manufacture: Sensirion) that measures the flow rate of air delivered from the pressure buffer. A Flow-meter (model: SFM-3000-200-C, manufacturer: Sensirion) with capacity of ± 200 [L/minPa], update time of 0.5 [ms], span accuracy of ±1.5 [% m.v.] in typical , offset accuracy of ± 0.05 [L/min] in typical, is used to measure the flow rate.

"The Permeation Evaluator" can supply and exhaust air by connecting a pipe from "The Breathing air simulator". Figure 2 shows a photograph of the "The Breathing air simulator". "The Breathing air simulator" can move air in and out by manually moving the piston horizontally. "The Breathing air

simulator" is equipped with a Flow-meter 2 (Model: SFM3000-200-C, manufacture: Sensirion) to measure the flow rate of air delivered from the piston cylinder. By pushing the piston, air discharged from the "The Breathing air simulator" flows in the order of the light blue arrows in Figure 1 and is discharged from the exhaust fan. Pulling the piston allows air to be sucked in through flow meters 1 and 2. The volume of the cylinder of "The Breathing air simulator" is 1.75 [L]. The direction of the air flow (flow rate $\boldsymbol{Q_1}$ and flow rate $\boldsymbol{Q_2}$) is indicated by the blue and red arrows in Figure 1.

The differential pressure in the pressure buffer relative to the outside air is measured by a differential pressure sensor (Model : SDP816-500 Pa, manufacture: Sensirion). The differential pressure can be changed by operating a fan on top of the device. The differential pressure $\boldsymbol{\Delta P}$ is positive when the pressure inside the pressure buffer is negative with respect to atmospheric pressure, since the inside of the pressure buffer is used as the reference. A differential pressure sensor (model: SPD-816-500Pa, manufacturer: Sensirion) with capacity of ± 500 [Pa], update time of 5 [m]s, span accuracy of ±3 [% m.v.], offset accuracy of ±0.1 [Pa], is used to measure the differential pressure. The differential pressure sensor and Flow-meter 1 and 2 are controlled by Arduino, which is controlled by a PC with measurement software. "Permeation Flow Rate Evaluator" is used to evaluate the differential pressure dependence of the transmitted flow rate of the measured object (nonwoven filter) by measuring the flow rate $\boldsymbol{Q}$ and differential pressure $\boldsymbol{\Delta P}$ with a flow meter and a differential pressure sensor.

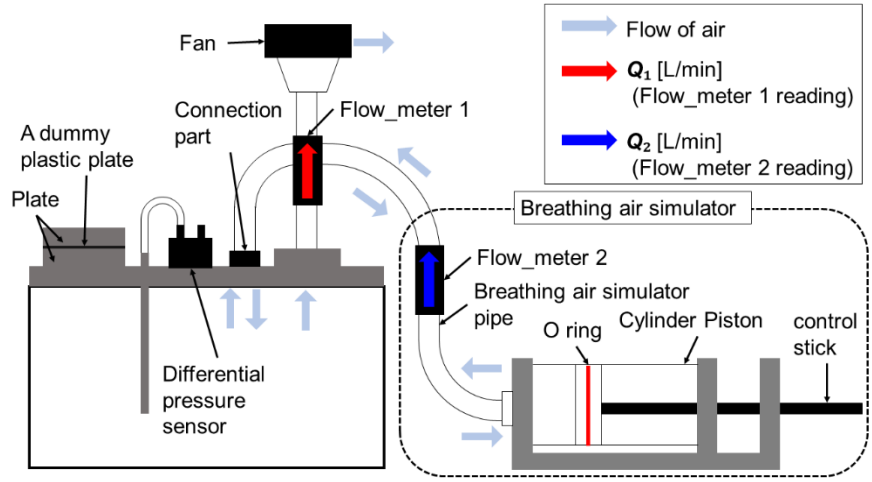

(a) Schematic diagram of "The Permeation Evaluator".

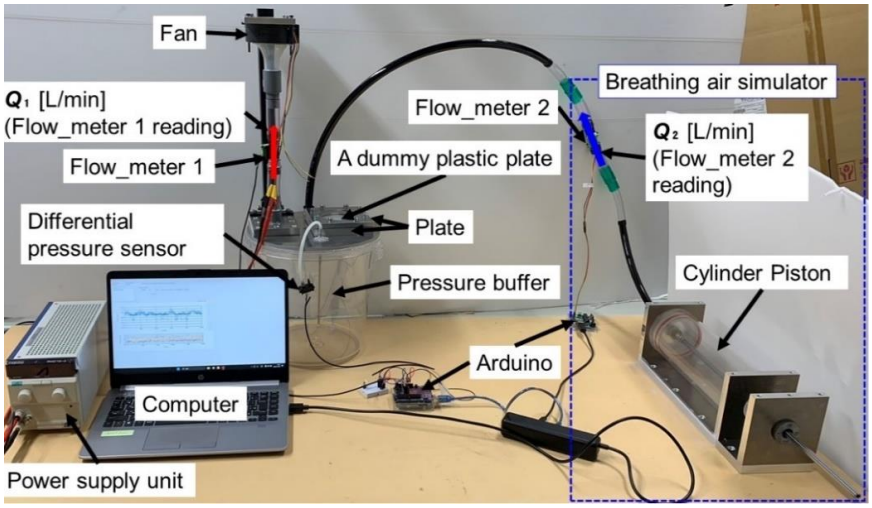

(b) Photograph of "The Permeation Evaluator".

Fig. 1. A Schematic and photograph diagram of "The Permeation Evaluator".

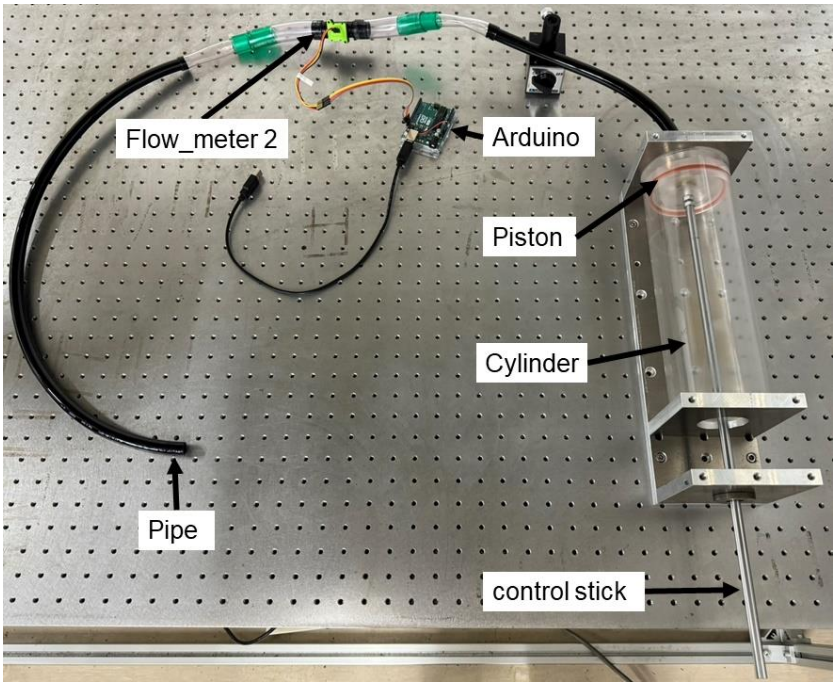

Fig. 2. A photograph of "The Breathing air simulator".

Figure 3 shows the measurement screen of the measurement software. The software displays time series of differential pressure, flow rate of Flow-meter 1, and flow rate of Flow-meter 2, and their average values. The measurement interval is fixed at 10 [ms] units. The number of measurements (number of samplings) can be adjusted in increments of one using Adjustment button of the number of measurements. Therefore, the measurement time is the number of measurements x 10 [ms]. After the measurement is completed, the screen displays a time series of differential pressure and flow rates of Flow-meter 1 and 2 and their average values.

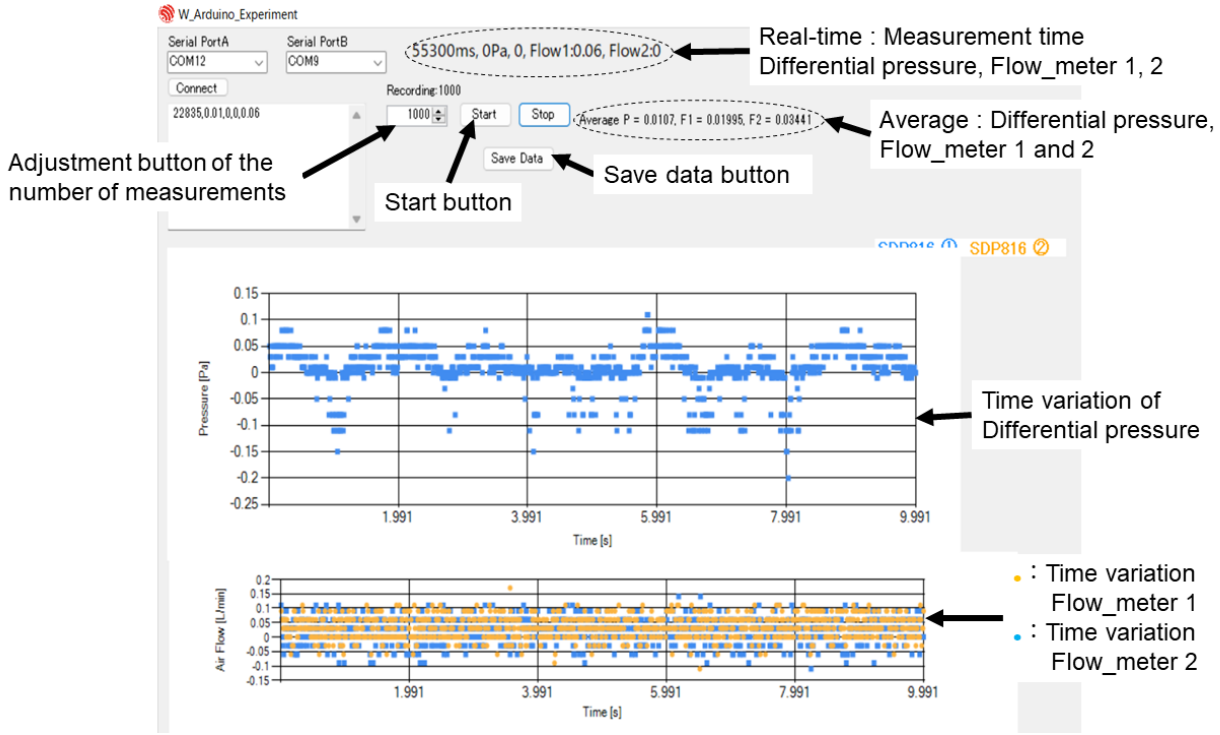

Fig. 3. A photograph of the measurement screen of the measurement software.

3. Leakage flow measurement of "The Permeation Evaluator"

3.1 Experimental equipment

Figure 1 shows the experimental equipment.

In the leakage measurement of the differential pressure dependence evaluation device, a vinyl packing to prevent leakage and a plastic plate to plug the hole are inserted between the plates and screwed on.

Figure 4 (a) shows a photograph of a vinyl packing sandwiched between plates, and Figure 4 (b) shows a photograph of a vinyl packing and a plastic plate to plug the holes between the plates (two aluminum plates with φ80 [mm] holes).

The hole for connecting the air pipe from the "The Breathing air simulator" should be blocked with a special dummy block.

(a) Vinyl sheet/packing

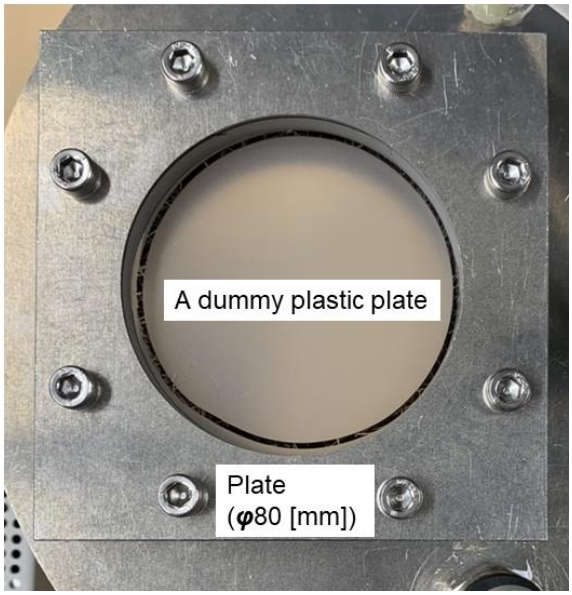

(b) Metal plates and the dummy plastic plate

Fig. 4. Photographs of plastic plates and vinyl packing sandwiched between the plates.

3.2 Experimental method

To evaluate the performance of the "Permeation Flow Rate Evaluator" the leakage flow rate of the device was measured, and the degree of leakage flow rate of the device was expressed by a regression equation.

The measurement procedure is described below.

- Place a vinyl packing and a plastic plate between the plates.
- Cover the hole where the air tube from the breathing simulator is connected. Tighten the screws for the plate using diagonal tightening.
- Activate the power supply unit to control the fan with voltage. The control range should be within ±500 Pa, which is the measurement range of the differential pressure gauge. Adjust the pressure gradually until the fan stops rotating (0 V).
- Measure the differential pressure $\boldsymbol{\Delta P}$ with the differential pressure gauge and the flow rate $\boldsymbol{Q_1}$ with the flow meter 1.
- The differential pressure $\boldsymbol{\Delta P}$ [Pa] and flow rate $\boldsymbol{Q_1}$ [L/min] measurements were averaged over a sampling interval of 10 [ms] and 1000 sampling points.

3.3 Experimental results

Figure 5 shows a graph with the average differential pressure ΔP on the horizontal axis and the average flow rate Q on the vertical axis.

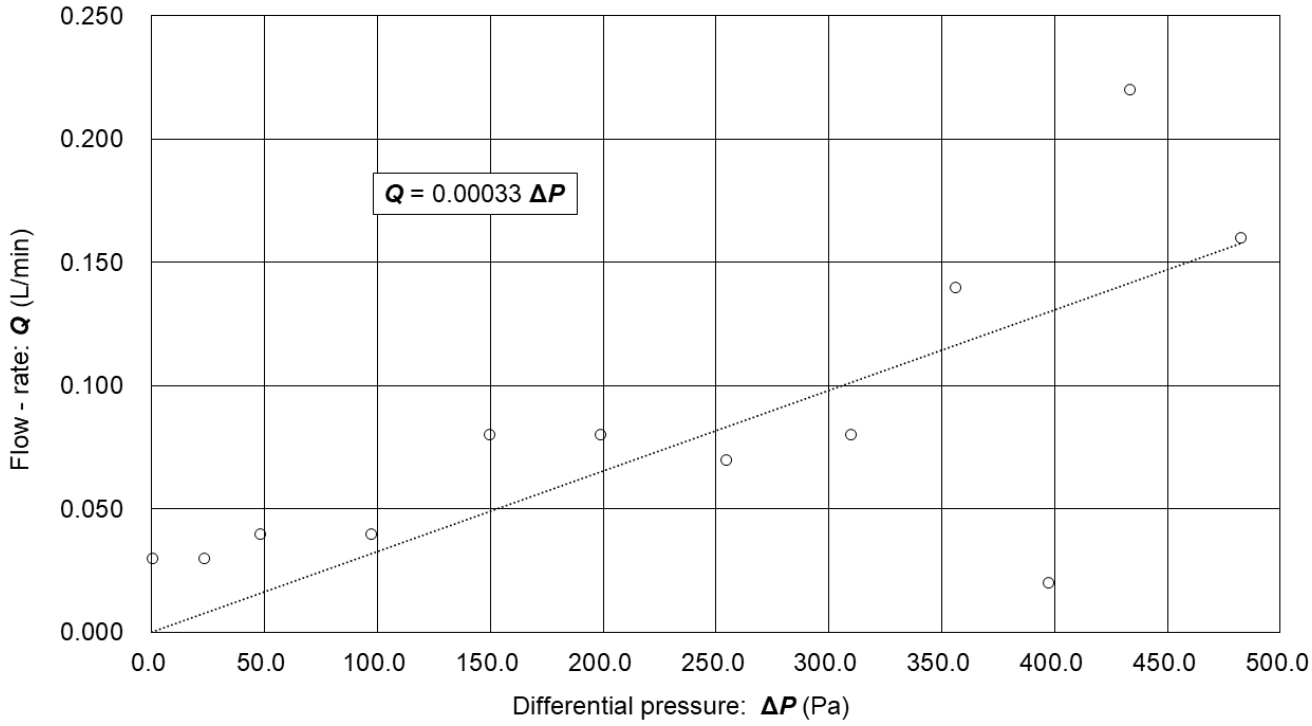

Fig. 5. Result of leakage flow measurement of "The Permeation Evaluator".

From Figure 5, the equation for the leakage of "The Permeation Evaluator" is $Q = 0.00033\,\Delta P$.

This regression equation represents the leakage of the differential pressure dependent evaluation device.

Furthermore, Figure 5 shows that the leakage flow rate of the "The Permeation Evaluator" is sufficiently small, about [0.05 L/min at 100 Pa] compared to the flow rate handled (up to 50 [L/min]). $Q_{measured} - Q_{estimated}$ was calculated using $Q_{estimated}$ as the estimated flow rate obtained by this equation and $Q_{measured}$ as the flow rate measured by the Flow-meter. The flow mean μ, standard deviation σ and RMS value of $Q_{measured} - Q_{estimated}$ and the flow mean μ, standard deviation σ and RMS value in the range of $Q_{measured}$ of $[Q_{measured} - Q_{estimated}] / [Q_{measured}]$ where $Q_{measured} > 0.05$ [L/min] are shown in Table 1.

Table. 1. The flow mean μ, standard deviation σ and RMS value of $Q_{measured} - Q_{estimated}$ [L/min] and $[Q_{measured} - Q_{estimated}] / [Q_{measured}]$.

$Q_{measured} - Q_{estimated}$ [L/min]			$[Q_{measured} - Q_{estimated}] / [Q_{measured}]$		
μ [L/min]	σ [L/min]	RMS value [L/min]	μ	σ	RMS value
0.01	0.04	0.04	0.04	0.20	0.20

4. Verification of flow measurement accuracy

4.1 Experimental equipment

Figure 1 shows a photograph and schematic diagram of the experimental equipment. Similar to the leakage flow measurement in the "The Permeation Evaluator" this experiment also involves placing a vinyl packing and a plastic plate between the plates, as shown in Figure 4.

Connect the "The Breathing air simulator" to the "The Permeation Evaluator" and apply a disturbance flow rate to the pressure buffer while changing the speed at which the piston is moved, and measure the degree of agreement between the given disturbance flow rate $\boldsymbol{Q_2}$ and the exhaust flow rate $\boldsymbol{Q_1}$ from the pressure buffer. Air is sucked into and exhausted from the “Breathing air simulator” to the “Permeation Flow Rate Evaluator” and the flow rates $\boldsymbol{Q_1}$ and $\boldsymbol{Q_2}$ measured by flow meters 1 and 2 are compared.

4.2 Experimental method

As part of the performance evaluation of the "The Permeation Evaluator" a measurement is performed to demonstrate the reliability of the flow measurement.

Connect the "The Breathing air simulator" to the "The Permeation Evaluator" and apply a disturbance flow rate to the pressure buffer while changing the speed at which the piston is moved, and measure the degree of agreement between the given disturbance flow rate $\boldsymbol{Q_2}$ and the exhaust flow rate $\boldsymbol{Q_1}$ from the pressure buffer. The measurement procedure is described below.

- Insert vinyl packing and plastic plates between the plates.
- Tighten the screws for the plates diagonally.
- Insert the air pipe from the breathing simulator.
- Set the piston at a position slightly away from the end, pull the piston from the initial position to the end of the device (preliminary movement), push the piston to the end (Exhaust movement), and then pull the piston to the end (Intake movement).
- This series of movements is considered as one set, and the differential pressure $\boldsymbol{\Delta P}$ is measured to be within ±500 Pa, and the flow rate $\boldsymbol{Q_1}$ and $\boldsymbol{Q_2}$ are measured.
- The speed at which the piston moves should be high (1±0.1 [s]), middle (2±0.1 [s]), and low (3±0.1 [s]) for each stroke.
- Measurements are taken 10 times at each speed.

4.3 Experimental results

Figures 6-8 show graphs of the time variation of the differential pressure $\boldsymbol{\Delta P}$ [Pa], flow rate $\boldsymbol{Q_1}$ [L/min], and flow rate $\boldsymbol{Q_2}$ [L/min] for one of the measured data. Figure 6 shows the piston moving at high speed (1±0.1 [s]), Figure 7 at middle speed (2±0.1 [s]), and Figure 8 at low speed (3±0.1 [s]).

Figures 6-8 show the time variation of the differential pressure $\boldsymbol{\Delta P}$ [Pa] and the flow rates $\boldsymbol{Q_1}$ [L/min] and $\boldsymbol{Q_2}$ [L/min] over the entire measurement in (a), the time variation in the Exhaust section in (b), and the time variation in the Intake section in (c). However, in (b) and (c), the pressure oscillation after the point where the differential pressure $\boldsymbol{\Delta P}$ [Pa] at the end of the stroke became positive for exhaust and negative for intake, respectively, was excluded from the measurement range, and $\boldsymbol{Q_1}$ >10 [L/min] during the Exhaust section and $\boldsymbol{Q_1}$ < -10 [L/min] during the Intake section were set as the measurement range. The start point of Exhaust section and Intake section was the point five measurements before the point at which the differential pressure $\boldsymbol{\Delta P}$ [Pa] exceeded ±1 [Pa], respectively. The end point was five measurement points after the point where the differential pressure $\boldsymbol{\Delta P}$ [Pa] became positive for exhaust air and negative for intake air, respectively.

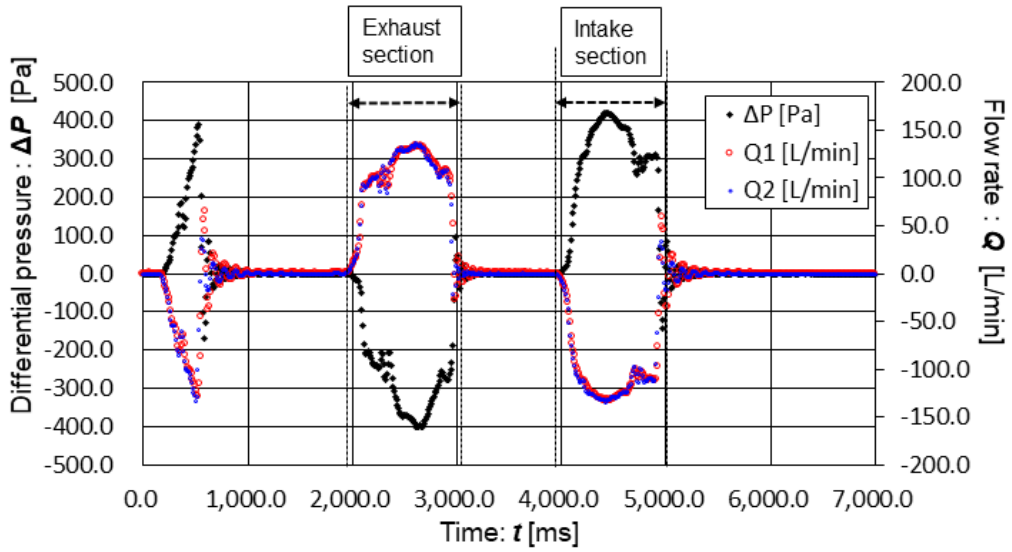

(a) Time variation of each flow rate throughout the experiment.

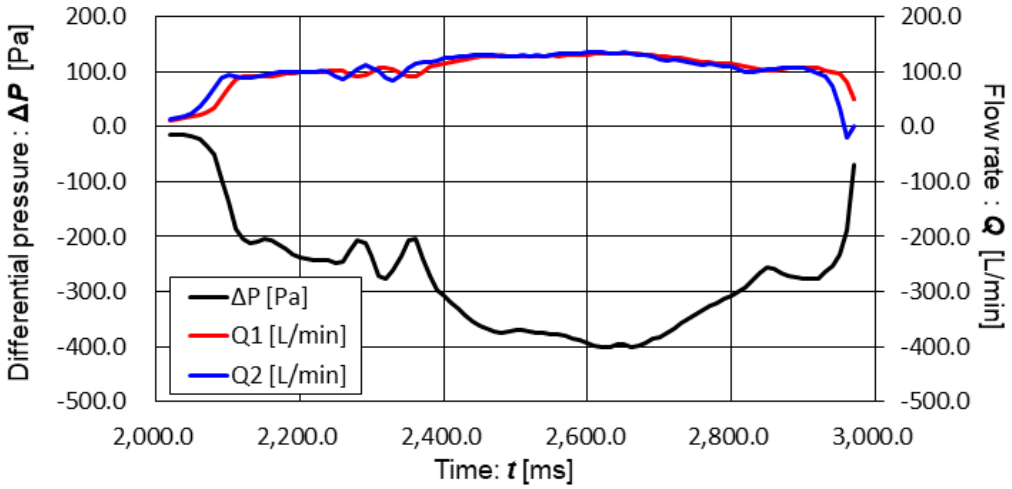

(b) Time change of Exhaust section for each flow rate.
(Only points used in the analysis)

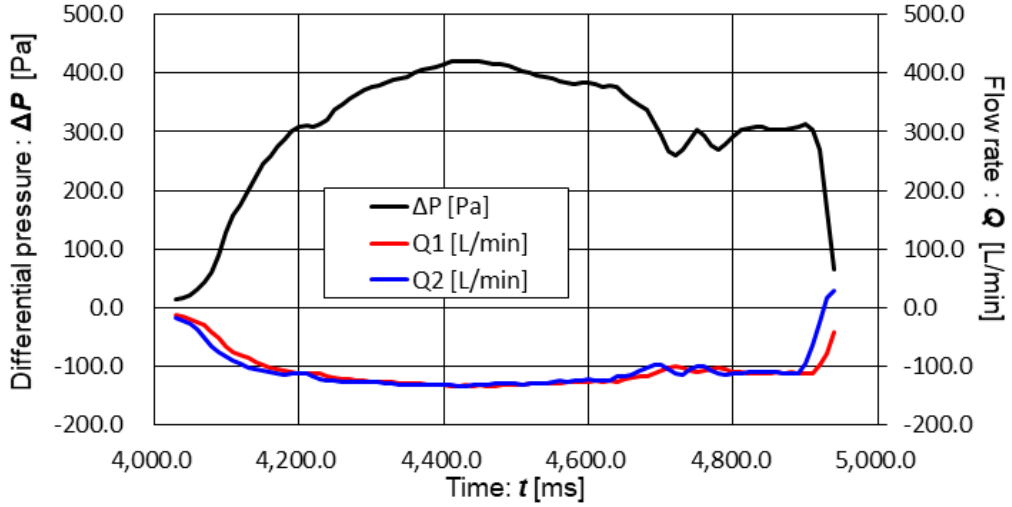

(c) Time change of Intake section for each flow rate.
(Only points used in the analysis)

Fig. 6. The time variation of ΔP [Pa] and Q_1 and Q_2 [L/min]. High speed mode: Period of each stroke (supply and exhaust) = 1±0.1 [s].

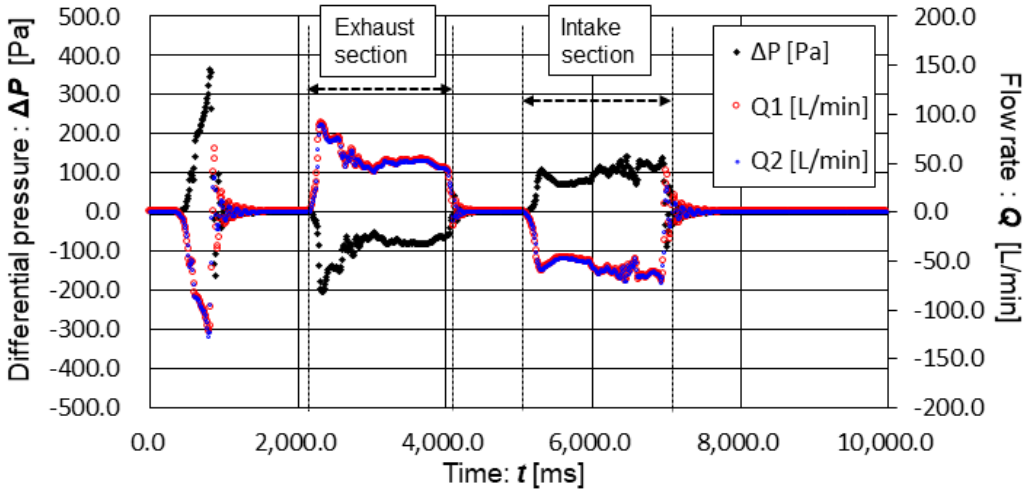

(a) Time variation of each flow rate throughout the experiment.

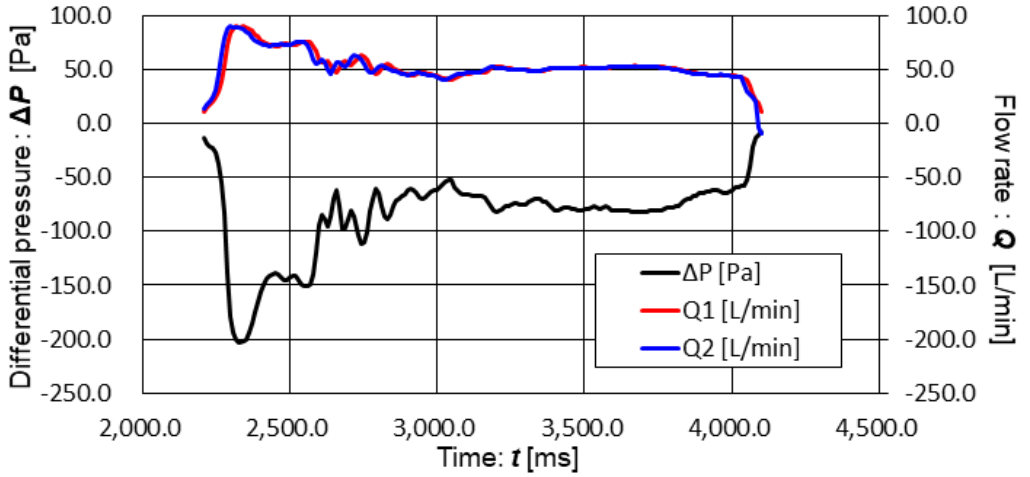

(b) Time change of Exhaust section for each flow rate.
(Only points used in the analysis)

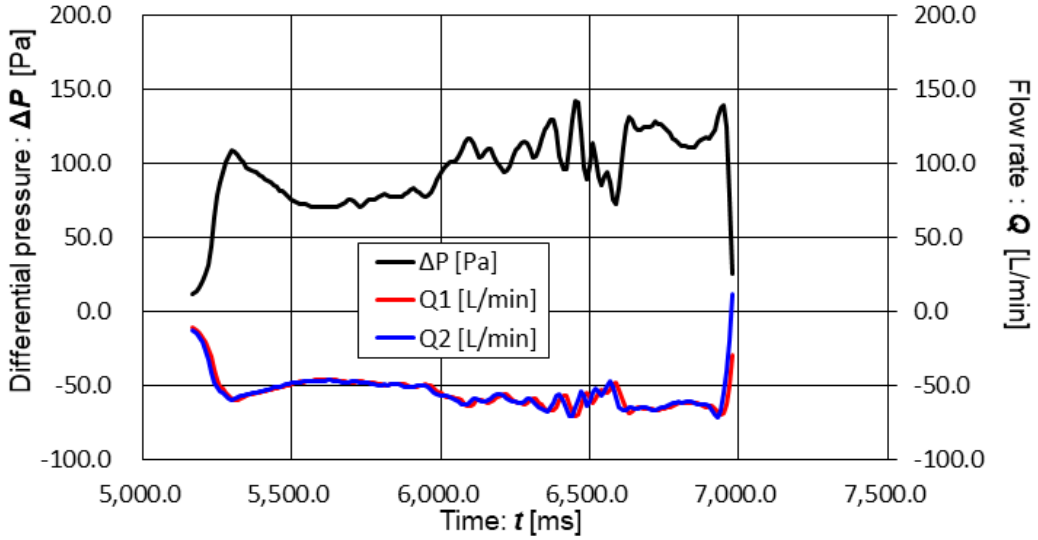

(c) Time change of Intake section for each flow rate.
(Only points used in the analysis)

Fig. 7. The time variation of ΔP [Pa] and Q_1 and Q_2 [L/min]. Middle speed mode: Period of each stroke (supply and exhaust) = 2±0.1 [s] .

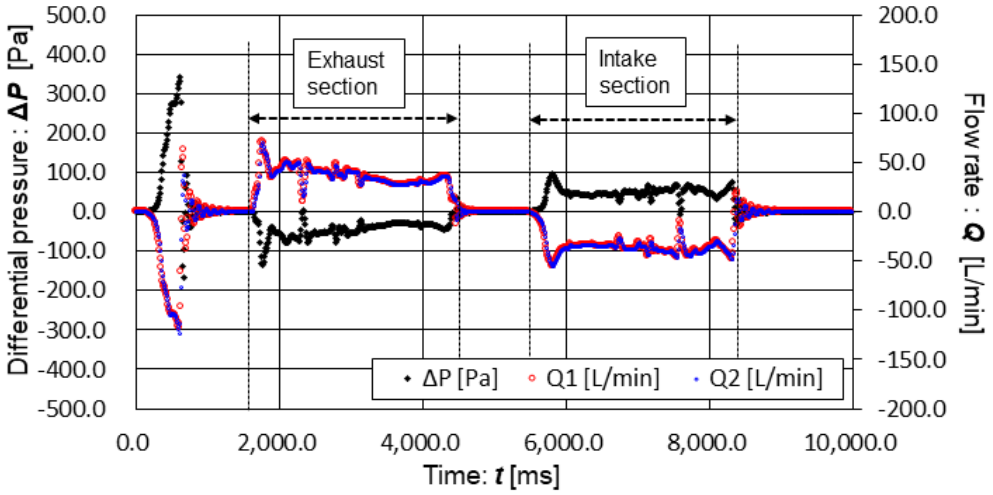

(a) Time variation of each flow rate throughout the experiment.

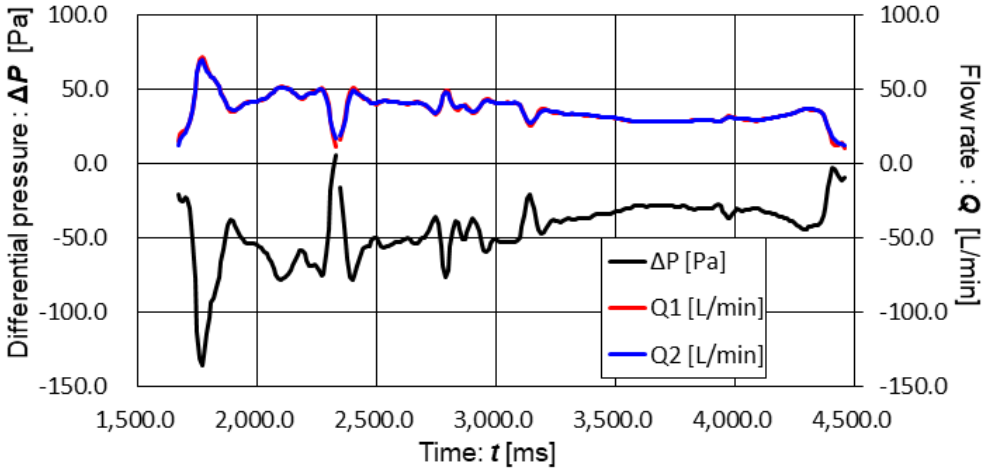

(b) Time change of Exhaust section for each flow rate.
(Only points used in the analysis)

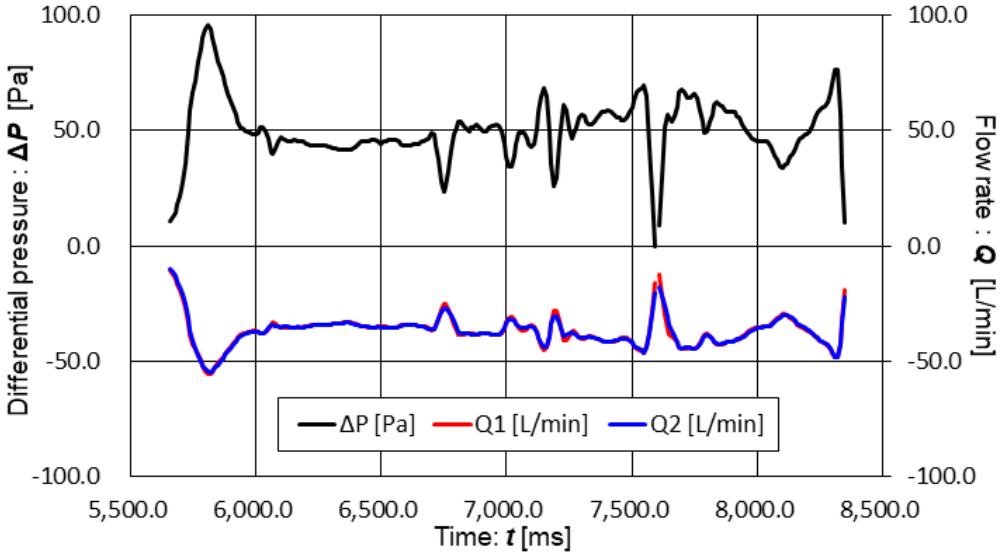

(c) Time change of Intake section for each flow rate.
(Only points used in the analysis)

Fig. 8. The time variation of ΔP [Pa] and Q_1 and Q_2 [L/min]. Low speed mode: Period of each stroke (supply and exhaust) = 3±0.1 [s].

Figure 9 below shows the mean and standard deviation of Q_1 [L/min] and Q_2 [L/min] for Exhaust section and Intake section, respectively, for the data measured 10 times at each speed.

The data points used were in the range of Q_1 >10 [L/min] in the Exhaust section and Q_1 < -10 [L/min] in the Intake section.

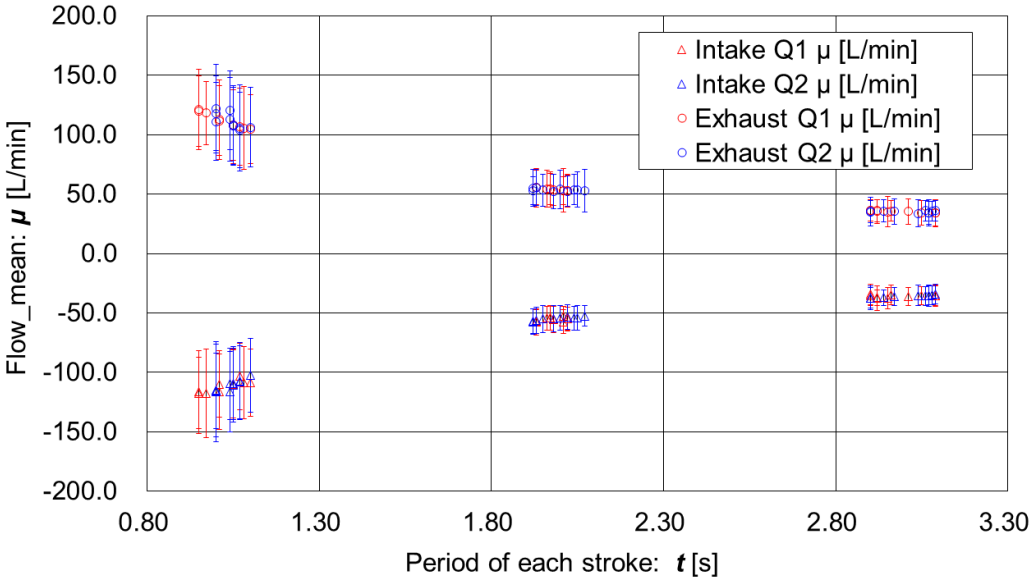

Fig. 9. Mean and standard deviation of Q_1 and Q_2.

Figure 9 shows that the slower the piston is moved, the smaller the absolute value of the mean flow velocity μ is, and the slower the piston is moved, the smaller the standard deviation is.

$Q_1 - Q_2$ [L/min] and $[Q_1 - Q_2] / Q_1$ were calculated from the measured Q_1 and Q_2. Figures 10 and 11 below show the mean and standard deviation of $Q_1 - Q_2$ [L/min] and $[Q_1 - Q_2] / Q_1$, respectively, for the Exhaust and Intake sections of the data measured 10 times at each speed.

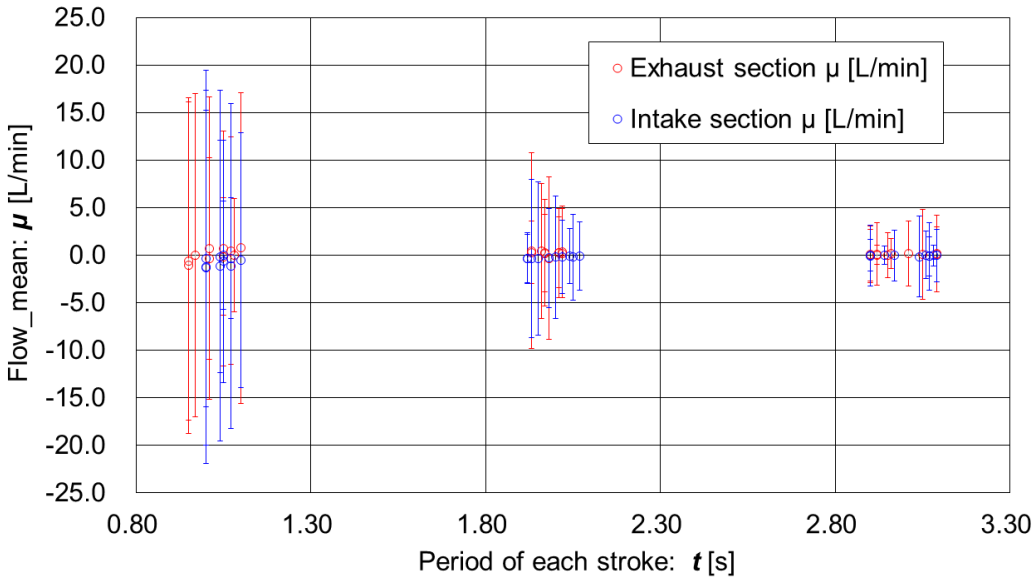

Fig. 10. Mean and standard deviation of $Q_1 - Q_2$ [L/min].

Figure 10 shows that the slower the piston is moved, the smaller the standard deviation is overall. It can also be seen that the slower the piston is moved, the more stable the mean μ value of the velocity difference is close to 0 [L/min].

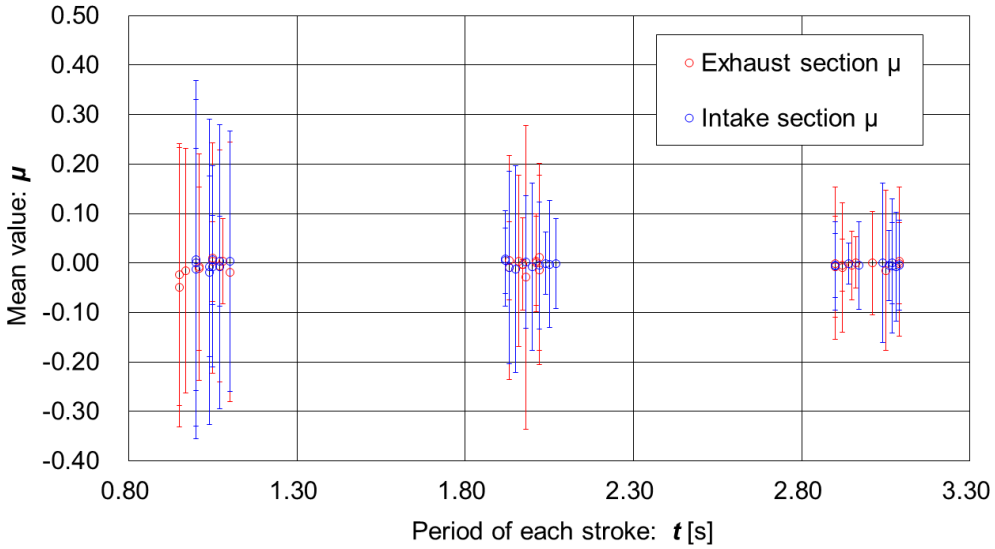

Fig. 11. Mean and standard deviation of $[Q_1 - Q_2] / Q_1$

Figure 11 shows that the slower the piston is moved, the smaller the standard deviation is overall. It can also be seen that the slower the piston is moved, the more stable the mean μ is close to 0.

Table 2 shows a table summarizing the average of 10 measurements of the flow rate mean μ, standard deviation σ, and RMS value for $Q_1 - Q_2$ [L/min] and $[Q_1 - Q_2] / Q_1$. Both $Q_1 - Q_2$ [L/min] and $[Q_1 - Q_2] / Q_1$ were measured in the range of Q_1 >10 [L/min] in the Exhaust section and Q_1 < -10 [L/min] in the Intake section, excluding the pressure oscillation value.

Table. 2. $Q_1 - Q_2$ [L/min] and $[Q_1 - Q_2] / Q_1$ flow rate mean μ, standard deviation σ, average of 10 measurements of RMS value.

		$Q_1 - Q_2$ [L/min]			$[Q_1 - Q_2] / Q_1$		
Speed	Section	μ [L/min]	σ [L/min]	RMS value [L/min]	μ	σ	RMS value
High	Intake	-1.11	14.10	14.12	-0.0031	0.24	0.24
	Exhaust	0.53	13.07	13.08	-0.011	0.21	0.21
Middle	Intake	-0.25	4.82	4.83	-0.0022	0.13	0.13
	Exhaust	0.25	5.69	5.70	-0.0030	0.15	0.16
Low	Intake	-0.046	2.48	2.48	-0.0040	0.093	0.092
	Exhaust	0.092	2.90	2.90	-0.0039	0.11	0.11

5. Discussion

5.1 Uncertainty in estimating the differential pressure dependence of flow rate

According to the datasheet, the accuracy of the flow meter is as follows,
[1] Span accuracy is ±1.5 [% m.v.] in typical
[2] Offset accuracy is ± 0.05 [L/min]. This is 0.5 [%] when the flow rate is 10 [L/min]
A standard uncertainty of flow rate measurement using the flow meter is estimated as follows,
$(1.5^2 + 0.5^2) \times 0.5 = 1.6$ [%] of the measured value, which is equal to or larger than 10 [L/min].

According to the datasheet, the accuracy of the flow meter is as follows,
[1] Span accuracy is ±3 [% m.v.]
[2] Offset accuracy is ± 0.1 [Pa]. This is 1 [%] when the flow rate is 10 [Pa]
A standard uncertainty of flow rate measurement using the flow meter is estimated as follows,
$(3^2 + 1^2) \times 0.5 = 3.2$ [%] of the measured value, which is equal to or larger than 10 [Pa].

5.2 Uncertainty evaluation of the leakage estimation equation of "The Permeation Evaluator"

From Table 1, the RMS value of [$\boldsymbol{Q}_{\mathbf{estimated}} - \boldsymbol{Q}_{\mathbf{measured}}$] / [$\boldsymbol{Q}_{\mathbf{measured}}$] is 0.20. The standard uncertainty in determining $\boldsymbol{Q}_{\mathbf{measured}}$ with the leakage flow estimation equation $\boldsymbol{Q} = 0.00033\,\Delta\boldsymbol{P}$ for the differential pressure dependent evaluation device is obtained by the equation (1).

$$\sqrt{[RMS\ value\ of\ [\boldsymbol{Q}_{\mathbf{estimated}} - \boldsymbol{Q}_{\mathbf{measured}}]/\boldsymbol{Q}_{\mathbf{measured}}]^2 + 0.016^2} \quad (1)$$

The standard uncertainty is 0.20.

5.3 Future Prospects

I agree with the Reviewer's comment that the next step in developing better Personal Protective Equipment (PPE) in a pandemic would be to scale up the technology and field test it in a variety of real-world scenarios.

Furthermore, the authors believe that it is necessary to identify problems and make further improvements through more quantitative evaluations of the high-performance, low-cost PAPR "Distancing-Free Mask" which is being developed by the authors as an alternative method of lockdown. "The Permeation Evaluator" and "The Breathing Air Simulator" developed in this study are expected to be useful tools for more precise and multifaceted quantitative evaluation.

In the future, we believe it is necessary we will conduct field tests in various real-world scenarios to identify problems and improve the "Distancing-Free Mask" through more quantitative evaluations.

6. Conclusion

The authors are developing a powered air-purifying respirator (PAPR) as a high-performance, inexpensive, and comfortable powered air-purifying respirator as an alternative to lockdown, with the aim of building a society that does not require lockdown.

The performance of the "The Permeation Evaluator" a device developed by the research group to evaluate the differential pressure dependence of the transmitted flow rate of nonwoven filters, was evaluated.

The leakage of "The Permeation Evaluator" was evaluated using the estimation equation $\boldsymbol{Q} = 0.00033\,\Delta\boldsymbol{P}$ with a standard uncertainty of 0.20. This value indicates the degree of leakage flow of the device.

Furthermore, the "The Breathing Air Simulator" was connected to a "The Permeation Evaluator" to provide a disturbance flow rate while changing the speed at which the piston was moved, and the reliability of the flow rate measurement was determined from the degree of agreement between the given disturbance flow rate $\boldsymbol{Q}_2$ and the exhaust flow rate $\boldsymbol{Q}_1$ from the pressure buffer. The RMS values of $[\boldsymbol{Q}_1 - \boldsymbol{Q}_2]/\boldsymbol{Q}_1$ were obtained in the range of $\boldsymbol{Q}_1 > 10$ [L/min] in the Exhaust section and $\boldsymbol{Q}_1 < -10$ [L/min] in the Intake section, resulting in the values in Table 2. This value indicates the reliability of the flow measurement in the range of $\boldsymbol{Q}_1 > 10$ [L/min] in the Exhaust section and $\boldsymbol{Q}_1 < -10$ [L/min] in the Intake section.

Funding

This research is funded by Japan Society for the Promotion of Science, Promotion of Joint International Research, KAKENHI (Grants-in-Aid for Scientific Research for FY2021, Issue No. 21KK0080).

Acknowledgements

The authors thank Prof. Naoya Ohta, Prof. Noriaki Yoshiura, Prof. Akihiro Takita, Prof. Seiji Hashimoto, Prof. Takao Yamaguchi, Prof. Kenji Amagai, Prof. Haruo Kobayashi, Prof. Shu Dong Wei, Prof. Osamu Takaki for their fruitful discussions.

References

[1] J. D. Sachs, S. S. A. Karim, L. Aknin, J. Allen, K. Brosbøl, F. Colombo, G. C. Barron, M. F. Espinosa, V. Gaspar, A. Gaviria, A. Haines, P. J. Hotez, P. Koundouri, F. L. Bascuñán, J. K. Lee, M. A. Pate, G. Ramos, K. S. Reddy, I. Serageldin, J. Thwaites, V. V.Freiberga, C. Wang, M. K. Were, L. Xue, C. Bahadur, M. E. Bottazzi, C. Bullen, G. L-Adjei, Y. B. Amor, O. Karadag, G. Lafortune, E. Torres, L. Barredo, J. G. E. Bartels, N. Joshi, M. Hellard, U. K. Huynh, S. Khandelwal, J. V. Lazarus and S. Michie, "The Lancet Commission on lessons for the future from the COVID-19 pandemic" The Lancet Commissions, Vol.400, Issue.10359, pp.1224-1280, 2022. showPdf (thelancet.com)

[2] T. Gobikannana, S.J. Pawarb, S. Kubera Sampath Kumarc, Md. Vaseem Chavhand, Amin Hirenbhai Navinbhaia and C. Prakash, "Importance of Antiviral and Antibacterial Face Mask Used in Pandemics: An Overview", Journal Of NLatural Fibers, Vol.20, No.1, pp.1-20, 2023. Importance of Antiviral and Antibacterial Face Mask Used in Pandemics: An Overview (tandfonline.com)

[3] A. Licina, A. Silvers, and L. Stuart, "Use of powered air-purifying respirator (PAPR) by healthcare workers for preventing highly infectious viral diseases—a systematic review of evidence", Systematic Review Update, 9, Article number;173, 2020.
Use of powered air-purifying respirator (PAPR) by healthcare workers for preventing highly infectious viral diseases—a systematic review of evidence | Systematic Reviews | Full Text (biomedcentral.com)

[4] T. Kiyonari, K. Goto, Y. Shizuno, A. Takita, R. M. Galindo and Y. Fujii, "Measurement of permeation flow-rate dependence on the differential-pressure and pump-voltage for the air-supply unit of the Distancing-Free Mask prototype", Proceedings of ICTSS2023 (Kiryu, Japan) December 2023.
https://conf.e-jikei.org/ICTSS/2023/proceedings/materials/proc_files/IPS01/ICTSS2023_IPS01_02_Kiyonari.pdf

[5] K. Goto, T. Kiyonari, Y. Shizuno, A. Takita, R. M. Galindo and Y. Fujii, "Measurement of permeation flow-rate dependence on the differential-pressure for the exhaust unit of Distancing-Free Mask prototype", Proceedings of ICTSS2023 (Kiryu, Japan) December 2023.
https://conf.e-jikei.org/ICTSS/2023/proceedings/materials/proc_files/IPS01/ICTSS2023_IPS01_03_GOTO_KAITO.pdf

[6] R. M. Galindo, A. Takita, E. Carcasona, E. Magalang, T. S. Galindo, S. Hashimoto, T. Yamaguchi, E. U. Tibay, D. W. Shu, H. Kobayashi, K. Amagai, N. Ohta, N. Yoshiura, A. Kuwana, A. Yano and Y. Fujii, "Low-Cost Powered Air-Purifying Respirator (PAPR) "Distancing-Free Mask Frontline (DFM-F) Prototype No.1" for the Operational Tests in Hospitals in Cebu City, Philippines", Journal of Mechanical and Electrical Intelligent System, Vol.5, No.2, pp.1-6, 2022.
http://jmeis.e-jikei.org/ARCHIVES/v05n02/JMEIS_v05n02a001.pdf

[7] E. Carcasona, R. M. Galindo, A. Takita, E. Magalang, T. S. Galindo, S. Hashimoto, T. Yamaguchi, E. U. Tibay, D. W. Shu, H. Kobayashi, K. Amagai, N. Ohta, N. Yoshiura, A. Kuwana, A. Yano and Y. Fujii, "Very-Low-Cost Powered Air-Purifying Respirator (PAPR) "Distancing-Free Mask Industry (DFM-I) Prototype No.1" and Proposal for a Lockdown-Free Industry", Journal of Technology and Social Science, Vol.6, No.2, pp.1-4, 2022.
http://jtss.e-jikei.org/issue/archives/v06n02/JTSS_v06n02a001.pdf

[8] Y. Fujii, “An Engineering Alternative to Lockdown During COVID-19 and Other Airborne Infectious Disease Pandemics: Feasibility Study”, JMIR Biomedical Engineering, Vol.9, 2024. https://biomedeng.jmir.org/2024/1/e54666/PDF

[9] Y.Fujii and A. Takita, " Booth-type of Personal Respiratory Air Purification Device: Distancing-Free Booth (Prototype No.1)", Journal of Mechanical and Electrical Intelligent System, Vol.4, No.2, pp.6-12, 2021. http://jmeis.e-jikei.org/ARCHIVES/v04n02/JMEIS_v04n02a002.pdf

[10] Y. Shizuno, T. Kiyonari, K. Goto, A. Takita, R. M. Galindo and Y. Fujii, “Measure ment of permeation flow-rate dependence on the differential-pressure for non-woven fab ric filters”, Proceedings of ICTSS2023 (Kiryu, Japan) December 2023. https://conf.e-jikei.org/ICTSS/2023/proceedings/materials/proc_files/IPS01/ICTSS2023_IPS01_01_Shizuno.pdf

[11] Stanislaw Dolny, Tomasz Rogozinski, “nonwoven filter fabric covered with microfiber layer used in wood dust separation”, Drewno, Vol. 57, No. 191, pp.125-134, 2014. https://bioresources.cnr.ncsu.edu/resources/creation-of-wood-dust-during-wood-processing-size-analysis-dust-separation-and-occupational-health/